Ultrahigh Molecular Weight Polyethylene/Polypropylene/ Organo-Montmorillonite Nanocomposites: Phase Morphology, Rheological, and Mechanical Properties

Jinggang Gai, Huilin Li

State Key Laboratory of Polymer Materials Engineering, Polymer Research Institute of Sichuan University, Chengdu, Sichuan 610065, People's Republic of China

Received 25 April 2007; accepted 9 June 2007
DOI 10.1002/app.26913
Published online 9 August 2007 in Wiley InterScience (www.interscience.wiley.com).

ABSTRACT: Phase morphology, rheological, and mechanical properties of ultrahigh molecular weight polyethylene (UHMWPE)/PP/organo-montmorillonite nanocomposites were investigated in this work. The results of TEM and XRD indicated that the organo-montmorillonite PMM prepared with the complex intercalator [2-methacryloyloxyethyldodecyldimethylammonium bromide/poly(ethylene glycol)] were exfoliated and dispersed into UHMWPE matrix, and the synergistic effect of the complex intercalator on the exfoliation and intercalation for montmorillonite occurred. Besides, the presence of PMM in UHMWPE matrix was found able to lead to a significant reduction of melt viscosity and enhancement in tensile strength and elongation at break of UHMWPE, except that izod-notched impact strength was without much obvious change. The dispersed PMM particles exhibited a comparatively large two-dimensional aspect ratio (L_{clay}/d_{clay} = 35.5), which played an important role in determining the enhancement of mechanical properties of UHMWPE nanocomposites. J Appl Polym Sci 106: 3023–3032, 2007

Key words: polyethylene; morphology; rheology; mechanical properties

INTRODUCTION

UHMWPE and its composites are widely used as bearing components, gears, guide rails, and medical material in total joint replacement[1–3] because of their excellent friction and wear characteristics, biocompatibility, chemical stability, effective impact load damping, and mechanical properties. Unfortunately, UHMWPE are either difficult or almost impossible to process in the melt because of their high melt viscosity, and much effort has been directed towards finding suitable processing methods.

The development of high-performance UHMWPE composites often involves the use of a low molecular weight solvent to reduce its high entanglement density in forming the final products. In 1980s, Smith and Lemstra[4–6] developed a commercial process of gel-spinning, with processing rates >10 m min^{-1}. This involved the dissolving of UHMWPE in decline at elevated temperatures followed by recrystallization, drawing of the resulting unentangled gel and drying. Subsequently, the fiber was hot drawn with the aim at inducing orientation. Further developments of this are swell drawing and die-free gel spinning.[7,8] All of these processing methods also involve significant quantities of solvents requiring removal and recycling. In the case of spinning this is of ~10 kg solvent/kg polymer.

Another effective way to reduce the melt viscosity is to dilute the UHMWPE with conventional PE (HDPE, LDPE, and LLDPE) that generally has a lower average molecular weight.[9,10] Small quantities of conventional polyethylene, however, do not improve the flow of UHMWPE sufficiently to render it amenable to conventional melt processing, while the mechanical and tribological properties of UHMWPE would decrease if effective amounts of conventional polyethylene were blended into it. Our previous investigation indicated that the addition of a small amount of PEG could also significantly reduce the die pressure and melt viscosity of UHMWPE/PP blend, but the tensile strength of the blend would sharply decrease when more than 2 phr PEG was added.[11]

Polymer-clay nanocomposites continue to be an area of great interest because of the many improvements in properties that these materials have over traditional composites.[12,13] It is generally assumed

Correspondence to: H. Li (nic7703@scu.edu.cn).
Contract grant sponsor: National Nature Science Foundation of China; contract grant number: 50233010.
Contract grant sponsor: National Basic Research Program of China; contract grant number: 2005CB623800.
Contract grant sponsor: Foundation of Doctoral Disciplines, Ministry of Education of China; contract grant number: 20030610057.

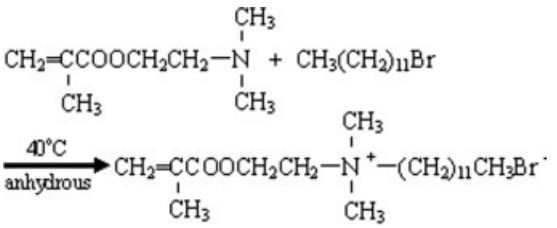

Figure 1 Scheme for the synthesis of MDAB.

that exfoliation of the clay is preferred for the greatest increases in nanocomposite properties. In the pristine state, layered silicates are only miscible with hydrophilic polymers. Unfortunately, the polymer in which natural clay is to be dispersed is often hydrophobic. The addition of surfactants lowers the surface energy of the inorganic host and improves the wetting characteristics of the polymer matrix, resulting in a larger interlayer spacing, and making the intercalation of many engineering polymers possible. UHMWPE/kaolin composites prepared by a polymerization-filling showed better dynamic rheological properties.[14] When the kaolin content was more than 15 wt %, the composite melts behaved like general polymer melts and could be extruded at low shear rate. When the kaolin content was less than 10 wt %, nevertheless, a common viscoelastic flow zone was absent from the flow curve of the composites. In addition, the stress vibration started at a low shear rate, and a coarse surface of the extrudate appeared.

In this article, the complex intercalator poly(ethylene glycol)/2-methacryloyloxyethyldodecyldimethylammonium bromide was used to modify Na^+-montmorillonite through ultrasonic irradiation. The influences of organo-montmorillonite (OMMT) content on the phase morphology, and properties of UHMWPE/PP/OMMT composites were also investigated.

EXPERIMENTAL

Materials

UHMWPE (M-II), with an average viscosity molecular weight of 2.5×10^6 and a mean particle diameter of about 300 μm, was supplied by Beijing No. 2 Auxiliary Agent Factory (Beijing, China). PEG was supplied by Liaoyang Aoke Chemical (Liaoning, China) with a molecular weight of 6000. PP (F401) was supplied by Lanzhou Chemical Industry Factory (Lanzhou, China) with a melt flow rate (MFR) of 2.0 g/10 min (230°C, 2.16 kg load). 2-(Dimethylamino)ethyl methacrylate (DM) and 1-bromododecane were supplied by Chengdu Kelong Chemical Reagents Factory (Chengdu, China). Ethyl acetate was supplied by Bodi Chemieals (Tianjin, China). Na^+-montmorillonite (MMT) was supplied by Zhejiang Fenghong clay Chemicals (Zhejiang, China).

Apparatus

The ultrasonic irradiation instrument is VC-1500 (Sonic and Material, USA) which has the following features: standard titanium horn with the diameter of 22 mm, adjustable power output, replaceable flat stainless steel tip, and digital thermometer to determine temperature. The power output was 9.54 W/cm^2 in this research.

Synthesis of surfactant MDAB for MMT modification

A cationic surfactant 2-methacryloyloxyethyldodecyldimethylammonium bromide (MDAB) was synthesized by the quaternarization reaction as shown in Figure 1. 2-(Dimethylamino)ethyl methacrylate and 1-bromododecane (1 : 1 molar ratio) reacted at 40°C for 80 h. The product is insoluble to either ingredient and thus precipitated. The white powder-like precipitant was purified by filtering and washing using ethyl acetate. It was then dried under vacuum at ambient temperature for 24 h.

Preparation of OMMT

OMMT was prepared by the ion exchange reaction. PEG (10 g) and MDAB (10 g) were first added to deionized water (800 mL) in order to form a uniform solution, to which the as-received MMT powders

TABLE I
(001) Diffraction Peaks, Corresponding *d*-spacing, h_{001}, and n_C of Various MMT and Their Composites

Samples	Peak position (°)	*d*-spacing (nm)	h_{001} (nm)	n_C
MMT	5.57	1.58	–	–
PM	4.75	1.86	–	–
MM	2.71	3.26	–	–
UHMWPE/PP/MM(90/10/5)	2.51	3.51	31.27	9.9
UHMWPE/PP/MM(90/10/3)	2.47	3.56	25.54	8.2
UHMWPE/PP/MM(90/10/1)	2.43	3.64	22.56	7.2
PMM	2.21	3.98	–	–
UHMWPE/PP/PMM(90/10/5)	No peak	Exfoliated	–	–
UHMWPE/PP/PMM(90/10/3)	No peak	Exfoliated	–	–
UHMWPE/PP/PMM(90/10/1)	No peak	Exfoliated	–	–

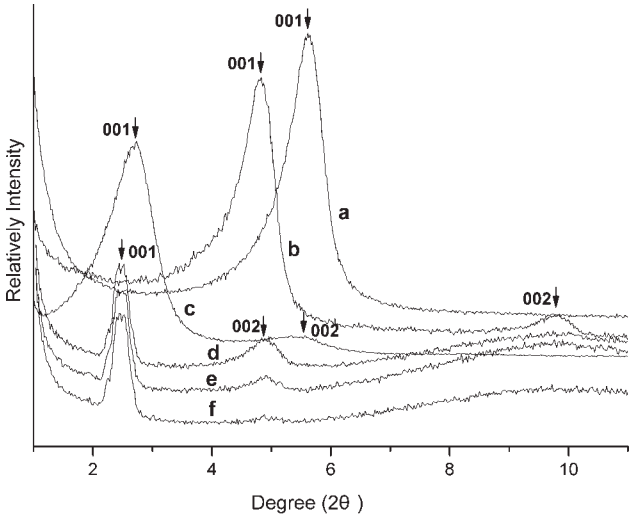

Figure 2 Wide-angle X-ray diffraction patterns: (a) MMT, (b) PM, (c) MM, (d) UHMWPE/PP/MM (90/10/5), (e) UHMWPE/PP/MM (90/10/3), and (f) UHMWPE/PP/MM (90/10/1).

were subsequently added. Next, the system was subjected to ultrasonic irradiation (acoustic intensity, 9.54 W/cm^2) for 1 h. Then, the exchanged MMT was filtered and redispersed in deionized water. This procedure was repeated several times until no bromide ion was detected with 0.1*N* $AgNO_3$ solutions. The filter cake was finally vacuum-dried at room temperature and crushed into powder. The OMMT is denoted as PMM. The preparation of other kinds of OMMT [PEG/MMT (PM) or MDAB/MMT (MM)] are similar with PMM.

Preparation of UHMWPE/PP/OMMT composites

The addition of OMMT (PMM, MM, or PM) was 1–5 parts per hundred parts of UHMWPE/PP (phr) by weight. UHMWPE was physically mixed with PP and OMMT, and then extruded by a general three-section single-screw extruder (D = 20 mm, L/D = 25). The temperatures were 190, 210, and 220°C for each section of the barrel and 210°C for the die. The extrudates were then made pellets and compression molded into 1 and 4 mm plates. Compression molding was carried out in the following conditions: preheated at 200°C for 5 min at low pressure, compressed for 5 min at 13 MPa at the same temperature, and then cooled to ambient temperature with the cooling rate 30°C/min in the mold at 13 MPa. Specimens for tensile test or izod-notched impact tests were got from the 1 and 4 mm plates, respectively.

Mechanical properties

Tensile tests were carried out at room temperature according to GB/T 1040-92 standard on Instron model 4302 machine (Instron, U.K.). Tensile strength, elongation at break, and yield strength were measured at a cross-head speed of 50 mm/min. Notched izod impact strength was measured with XJ-40AX (Wuzhong Material Testing Technical, China) at room temperature according to GB 1843-80 standard.

Transmission electron microscopy

Transmission electron microscopy (TEM) observations were carried out with an H-7100 (Tokyo, Japan) instrument with an accelerating voltage of 100 kV. The ultrathin sections with a thickness of 100 nm were microtomed in liquefacient nitrogen by a Reichert Ultracut cryoultramicrotome without staining.

Wide-angle X-ray diffraction

Wide-angle X-ray diffraction (WAXD) spectra were recorded with a Philip X'pert prd diffractometer (Japan). The X-ray beam was nickel-filtered Cu Ka (λ = 0.1542 nm) radiation operated at 40 kV and 100 mA. MMT, PM, MM, or PMM was studied as powders. Samples of UHMWPE composites were cut from 1 mm plates. The scanning range was varied from 2θ = 1°–11° with a rate of 5°/min.

Rheological experiments

The rheological measurements were carried out on a Gottfert Rheograph 2002 (Gottfert, Germany). The capillary diameter and its length-to-diameter ratio are 1 mm and 30, respectively. The die had an entrance angle of 180°. Entrance pressure losses were assumed to be negligible for such a long capillary

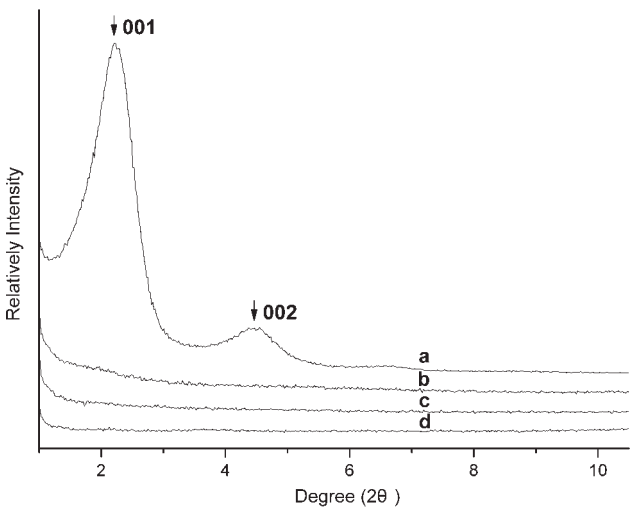

Figure 3 Wide-angle X-ray diffraction patterns: (a) PMM, (b) UHMWPE/PP/PMM (90/10/5), (c) UHMWPE/PP/PMM (90/10/3), and (d) UHMWPE/PP/PMM (90/10/1).

Figure 4 Transmission electron micrographs of UHMWPE/PP/MM (90/10/3).

die, and therefore no Bagley correction was applied. The flow properties of these specimens were measured at 200°C.

Polarizing optical microscopy

Polarized optical micrographs (POM) were taken on a Leitz Laborlux 12POL (Leitz, Germany) at 50× magnification. Samples were prepared through cutting small pieces from prepared films. Samples weighing 25 mg were melted on glass slides with coverslips to form thin films which were ~20–50 μm thick.

RESULTS AND DISCUSSION

Structure of OMMT platelets in the composites

The dispersion state and nanostructure of OMMT platelets in a polymer layered silicate nanocomposite (UHMWPE/PP/OMMT) have dramatic influences on its mechanical and rheological performances. The structure of the nanocomposites in the nanometer range has typically been elucidated using WAXD and TEM.

Figure 3 shows the respective X-ray diffraction traces for the MMT, PM, MM powders and various representative composites, exhibiting a shift of (001) diffraction peaks towards the lower diffraction angles in different manners. The (001) diffraction peak for PM powder is found to shift, in a comparatively short range, from $2\theta = 5.57^\circ$ ($d_{001} = 1.58$ nm) to 4.75° ($d_{001} = 1.86$ nm). On the other hand, the (001) diffraction peak for the MM powder shifts to $2\theta = 2.71^\circ$ ($d_{001} = 3.26$ nm) (Table I). With increasing clay content, these peaks (001) become stronger, and slightly shift towards higher diffraction angles, at 2.43° ($d_{001} = 3.64$ nm), 2.47° ($d_{001} = 3.56$ nm), and 2.51° ($d_{001} = 3.51$ nm) for UHMWPE/PP blended with 1, 3, and 5 phr MM, respectively (Fig. 2 and Table I). These shifts of the (001) diffraction peak are probably attributed to the intercalation of PEG, MDAB, PP, or UHMWPE chains snaking into silicate galleries.

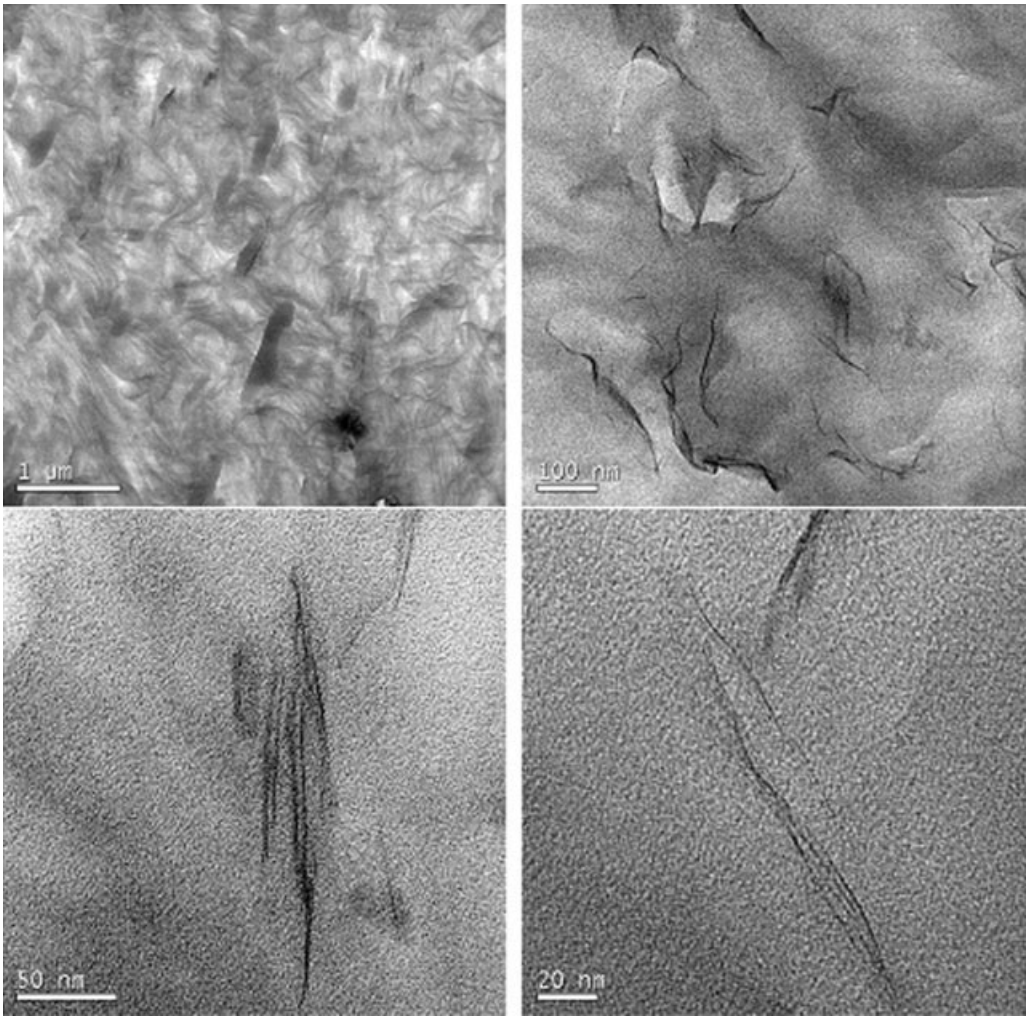

Figure 5 Transmission electron micrographs of UHMWPE/PP/PMM (90/10/3).

For PM, MM, UHMWPE/PP/MM (90/10/5), UHMWPE/PP/MM (90/10/3), and UHMWPE/PP/MM (90/10/1) samples respectively, sharp peaks observed at $2\theta = 9.79^\circ$, 5.54°, 4.93°, 4.90°, and 4.88° are confirmed to be (002) plane (d_{002}) (Fig. 2). The existence of the (001) and (002) diffraction peaks shows that the MM in the composites still retains an ordered structure after melt mixing despite that the interlayer spacing increased significantly compared to that of MM powder.

As it is shown in Figure 3 and Table I, the peak of (001) plane of PMM shifts to lower angle ($2\theta = 2.21^\circ$) when compared with those of PM or MM. After the melting process, the original (001) together with (002) diffraction peaks disappeared in the UHMWPE/PP/PMM (90/10/1), UHMWPE/PP/PMM (90/10/3), and UHMWPE/PP/PMM (90/10/5) composites in the range of $2\theta = 1^\circ$–11°. The disappearance established the formation of exfoliated and better intercalated structure for composites UHMWPE/PP/PMM, as opposed to an intercalated structure for UHMWPE/PP/PM and UHMWPE/PP/MM systems. The structure of PMM in the matrix is probably attributed to the synergistic effects of the complex intercalator (PEG/MDAB) on the intercalation and exfoliation for MMT.

From the WAXD patterns, the crystallite size normal to the (001) plane of the OMMT particles in UHMWPE matrix is calculated by the Scherrer equation,[15] written as

TABLE II
Some Characteristic Parameters of UHMWPE/PP/PMM (90/10/3) and UHMWPE/PP/MM (90/10/3) Obtained from TEM and WAXD Measurements

Characteristic parameters	UHMWPE/PP/PMM (90/10/3)	UHMWPE/PP/MM (90/10/3)
L_{clay} (nm)	241.5 ± 10	425.4 ± 16
d_{clay} (nm)	6.8	25.6
L_{clay}/d_{clay}	35.5	16.6

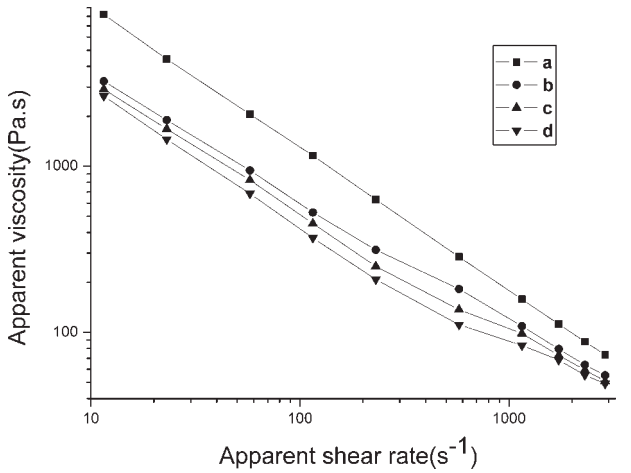

Figure 6 Plot of the logarithm of the apparent viscosity versus the logarithm of the apparent shear rate for (a) UHMWPE/PP (90/10), (b) UHMWPE/PP/PM (90/10/1), (c) UHMWPE/PP/PM (90/10/3), and (d) UHMWPE/PP/PM (90/10/5).

$$h_{001} = \frac{K\lambda}{\beta \cos \theta_{001}} \quad (1)$$

where K is a constant (= 0.91), λ the X-ray wavelength (= 0.154 nm), β the width of Bragg diffraction peak determined by the full width at haft maximum in radian unit, and θ_{001} the half of (001) diffraction angle. From the calculated crystallite size (h_{001}), i.e. the thickness of the dispersed clay, the actual number of layers, n_C, staked in a clay particle can be approximately calculated as follows[16]

$$n_C = \frac{h_{001}}{d_{001}} + 1 \quad (2)$$

Table I also shows the calculated value of h_{001} and n_C for the composites UHMWPE/PP/MM. The sample UHMWPE/PP/MM shows that the h_{001} and n_C values are in the range of 31.27–22.56 nm and 9.9–7.2 layers. Moreover, the thickness of the dispersed stacked silicate layers in the UHMWPE matrix gradually increases with MM loading. Therefore, it can be concluded that the well ordered intercalated MMT was formed after the melting process and coherence order of the silicate layers increased with increasing OMMT.

The internal structure of the clay in the nanometer scale was observed via TEM analysis. Figures 4 and 5 respectively show the typical TEM images of UHMWPE/PP/PMM (90/10/3) and UHMWPE/PP/MM (90/10/3) composites. Bright field is the image of polymer, in which dark entities are the cross-section of intercalated silicate layers.[17] Form factors such as average length L_{clay}, thickness ($d_{clay} \approx h_{001}$) of the dispersed clay particles can be obtained from TEM images[18] and the results are summarized in Table II. Combining the results of WAXD analysis and TEM observation, one can estimate another parameter L_{clay}/d_{clay}, the two-dimensional aspect ratio of the dispersed clay particles, which plays an important role in determining the enhancement of mechanical properties of UHMWPE nanocomposites.

For MM in the composites, one can observe large anisotropy of the stacked and flocculated silicate layers, whose original thickness is ~1 nm and average length ~100 nm (Fig. 4). The size of some of the flocculated silicate layers appears to reach about 425.4 nm in length (L_{clay}) and 25.6 nm in thickness (d_{clay}), owing to the hydroxylated edge–edge interaction of silicate layers. On the other hand, PMM exhibit less stacking (d_{clay} = 6.8 nm) of the silicate layers with L_{clay} of about 241.5 nm and are little orderly oriented in the matrix (Fig. 5).

Rheological behavior

The measurement of rheological property of polymer nanocomposites under molten state is crucial to gain fundamental understanding of relationship between the processability and structure of these materials. Generally, the rheological behavior of polymer nanocomposite melts strongly depends on their nanostructure, state of dispersion–distribution, and interfacial properties.[18,19]

The melts of pure UHMWPE flew unsteadily at lower shear rate, and no steady rheology data could be obtained at higher shear rates because of the pressure vibration. The effect of OMMT on the rheological properties of UHMWPE was also investigated, as is shown in Figures 6 and 7. These figures show

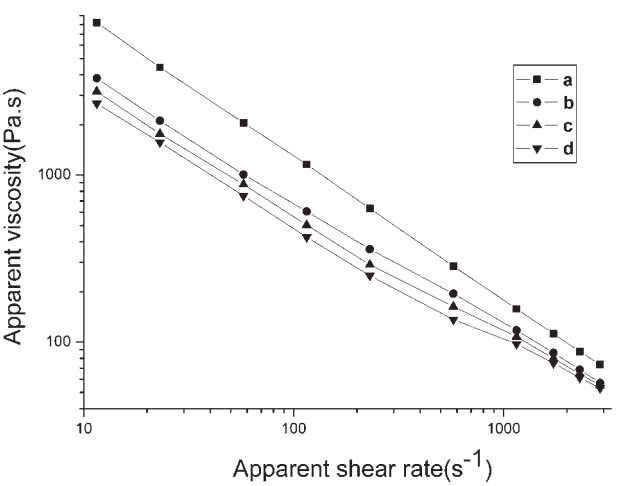

Figure 7 Plot of the logarithm of the apparent viscosity versus the logarithm of the apparent shear rate for (a) UHMWPE/PP (90/10), (b) UHMWPE/PP/PMM (90/10/1), (c) UHMWPE/PP/PMM (90/10/3), and (d) UHMWPE/PP/PMM (90/10/5).

TABLE III
The Mechanical Properties of Pure UHMWPE and its Composites

Sample	Tensile strength (MPa)	Elongation at break (%)	Yield strength (MPa)	Izod-notched impact strength (kJ/m2)
UHMWPE	38.71	396.41	25.85	No break
UHMWPE/PP(90/10)	39.16	431.22	26.02	No break
UHMWPE/PP/PM (90/10/1)	42.33	487.99	26.66	112.86
UHMWPE/PP/PM (90/10/3)	44.12	540.51	27.21	100.91
UHMWPE/PP/PM (90/10/5)	42.85	502.62	28.27	96.93
UHMWPE/PP/MM (90/10/1)	43.13	501.11	27.61	No break
UHMWPE/PP/MM (90/10/3)	44.83	521.35	28.13	No break
UHMWPE/PP/MM (90/10/5)	44.08	517.40	28.44	102.87
UHMWPE/PP/PMM (90/10/1)	44.67	477.98	27.33	No break
UHMWPE/PP/PMM (90/10/3)	46.52	505.88	27.39	No break
UHMWPE/PP/PMM (90/10/5)	47.55	546.19	27.85	No break

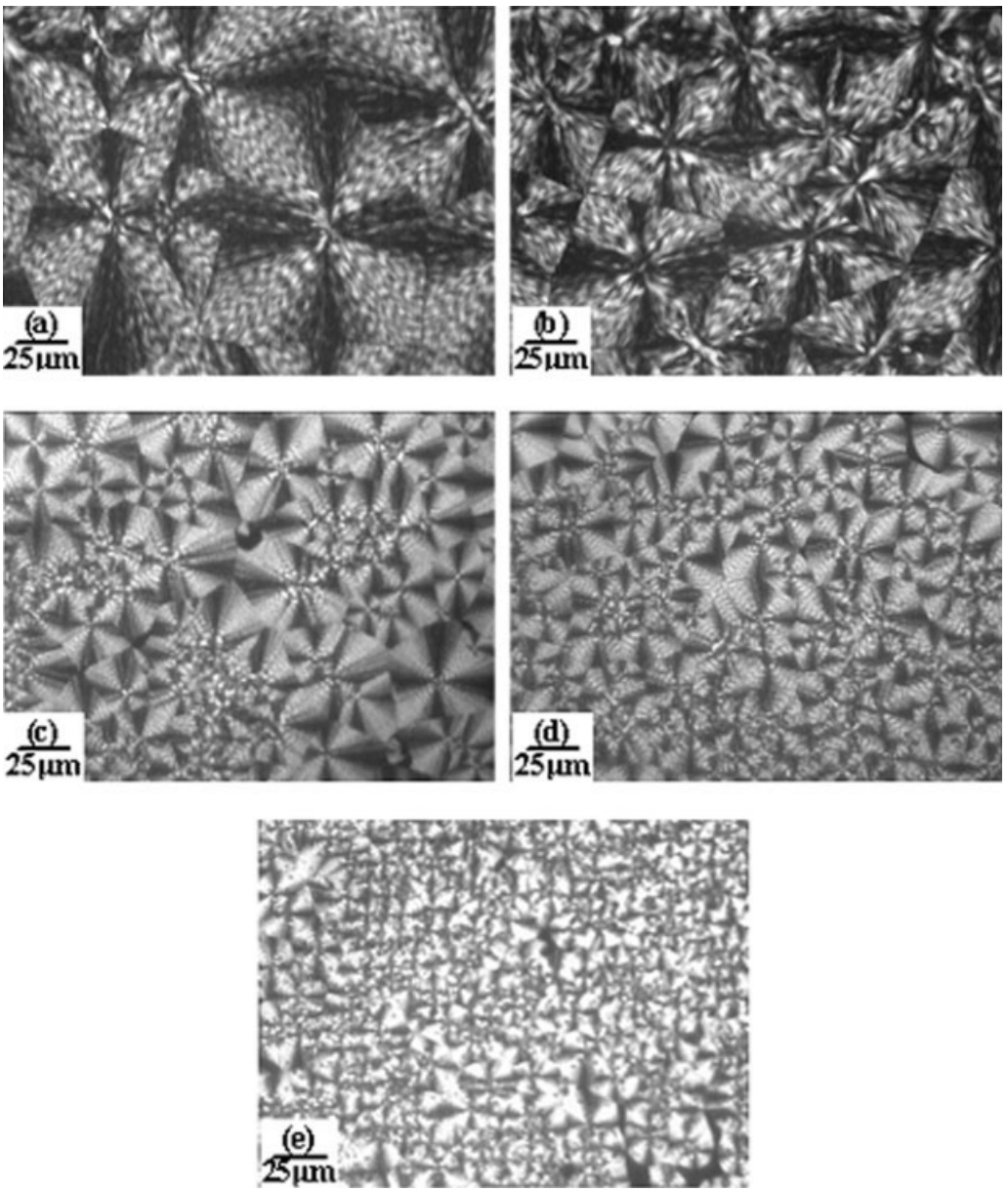

Figure 8 Optical micrographs of pure (a) UHMWPE, (b) UHMWPE/PP (90/10), (c) UHMWPE/PP/MM (90/10/1), (d) UHMWPE/PP/MM (90/10/3), and (e) UHMWPE/PP/MM (90/10/5).

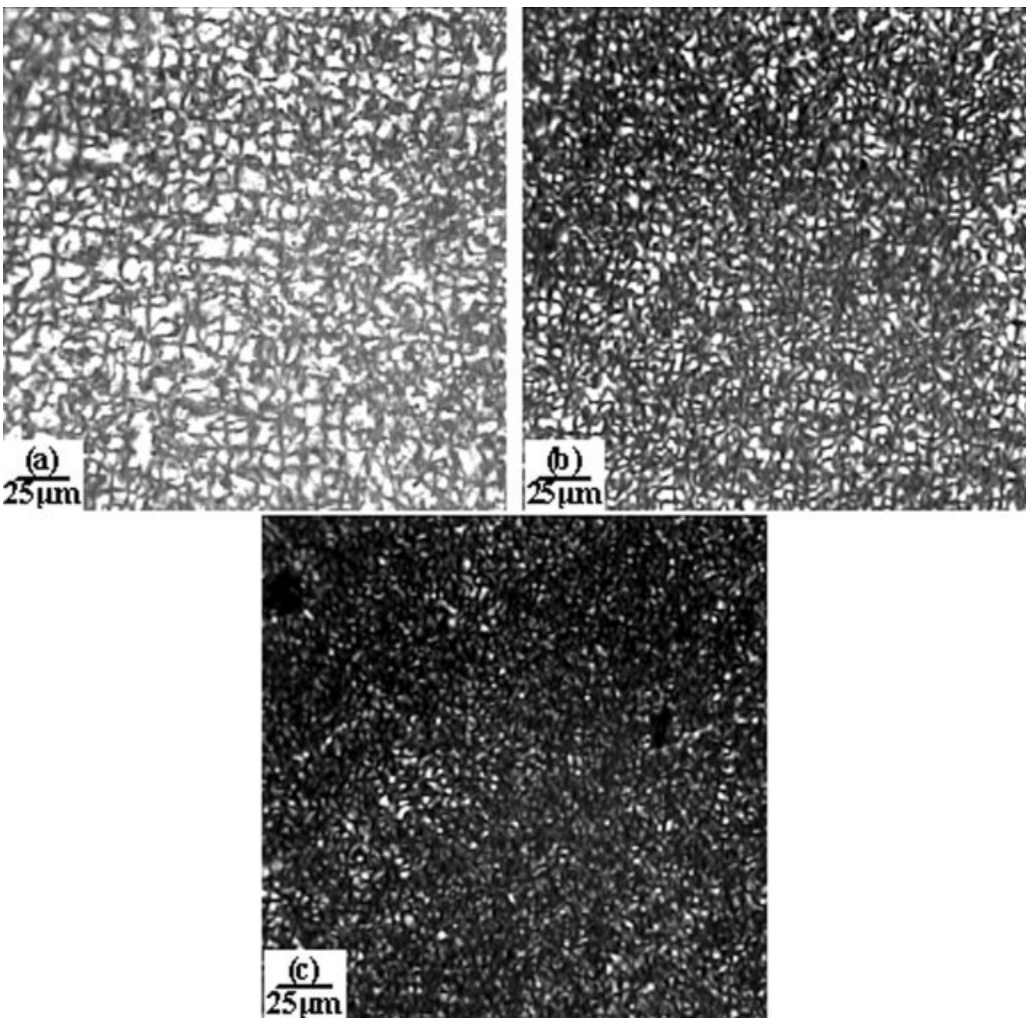

Figure 9 Optical micrographs of (a) UHMWPE/PP/PMM (90/10/1), (b) UHMWPE/PP/PMM (90/10/3), and (c) UHMWPE/PP/PMM (90/10/5).

that the viscosities of the UHMWPE/PP blend, UHMWPE/PP/PM, and UHMWPE/PP/PMM composites decrease with increasing shear rate, indicating a feature of pseudoplastic flow. These studies also show that the addition of OMMT (PM and PMM) can significantly reduce the apparent viscosity of the UHMWPE/PP (90/10) blend, and no pressure vibration occurs throughout the whole shear rate range investigated. Moreover, the viscosities of composites tend to decrease with increasing clay concentration (Figs. 6 and 7). A comparison of the flow behavior of UHMWPE/PP blend, UHMWPE/PP/PM, and UHMWPE/PP/PMM composites shows that the most obvious effect on the viscosity reduction of UHMWPE occurs in UHMWPE/PP/PM (90/10/5) (Figs. 6 and 7).

It is well known that PEG has very low viscosity and good lubricating property, and it is incompatible with UHMWPE and PP. Intercalated and exfoliated OMMT layers serve as a lubricant carrier in the UHMWPE/PP/OMMT composites. In other words, the short PEG chains on the surface of clay layers can act as an internal lubricant to induce interphase slippage of the blend. Finally, synergistic effect of PEG and MMT on reducing the viscosity is achieved.

Unlike PM and PMM, the addition of MM to the UHMWPE/PP blend results in a significant increase of melt viscosity, and no steady rheology data could be obtained at shear rates range investigated. The dramatic viscosity increase observed in UHMWPE/PP/MM system suggests a significant degree of silicate platelets dispersion in UHMWPE matrix.[20]

Mechanical properties

The mechanical properties of composites depend on many factors, including the aspect ratio of the filler, the degree of dispersion of the filler in the matrix, and the adhesion at the filler-matrix interface. Table III summarizes the mechanical properties of UHMWPE and its composites prepared with the var-

TABLE IV
The Average Diameters of Spherulites of Materials Studied

Sample	Average diameters of spherulites (μm)
UHMWPE	122.22
UHMWPE/PP (90/10)	66.67
UHMWPE/PP/MM (90/10/5)	38.89
UHMWPE/PP/MM (90/10/3)	27.78
UHMWPE/PP/MM (90/10/1)	22.22
UHMWPE/PP/PMM (90/10/5)	16.67
UHMWPE/PP/PMM (90/10/3)	12.50
UHMWPE/PP/PMM (90/10/1)	8.33

ious OMMT. In the case of the UHMWPE/PP (90/10) blend, its mechanical properties remain nearly unchanged when compared with pure UHMWPE.

The stress–strain curves for all of the samples are similar. With same MMT loading, the tensile strengths of samples with better dispersed PMM are higher than that of samples with more poorly dispersed PM or MM. For pristine UHMWPE, the tensile strength is 38.71 MPa. Addition of 5 phr of PMM increases the tensile strength to 47.55 MPa, which is 22.84% higher than that of the pristine UHMWPE. For PM or MM based system, tensile strength increases with 1–3 phr of clay loading. With 5 phr PM or MM content, however, the tensile strength starts to decrease, but they are still higher than those of the pure UHMWPE and UHMWPE/PP blend. This decrease of the mechanical properties can be attributed to the aggregation of the clay nanolayers in the matrix.

With the same OMMT, elongation at break of nanocomposite materials almost follows the same trend as the tensile strength. Broadly speaking, yield strength improves with the increase of clay loading, as shown in Table III. However, there are not notable differences in the level of yield strength improvement when different OMMT are used. For the UHMWPE/PP/PMM composites, izod-notched impact strengths are without much obvious change, but a slight drop of impact strengths for PM or MM based composites appears with higher clay loading.

As discussed earlier, the dispersion of the OMMT in UHMWPE/PP/PMM nanocomposites is better than that in UHMWPE/PP/PM and UHMWPE/PP/MM composites, so UHMWPE/PP/PMM composites are more effective than PM and MM based composites in reinforcement.

To further explain the variation of mechanical properties, the microscope crystal morphology of UHMWPE nanocomposites is investigated by polarizing light microscope analysis. Figures 8 and 9 show the typical spherulitic texture of UHMWPE and its composites. It is clearly seen that the spherulites in neat UHMWPE are larger than those in its blends and composites. The more concentrated OMMT is, the higher is the nucleation, which can be judged from the decreased size of spherulites and the increase of the average numbers of spherulite per unit area. For example, the maximum spherulite radius in UHMWPE/PP/MM decreases from 38.89 to 22.22 μm, and in UHMWPE/PP/PMM from 16.67 to 8.33 μm [Fig. 8(c–e) Fig. 9 and Table IV]. The dramatic changes of the average numbers and size of spherulite in nanocomposites result from an enhancement of spherulite nucleation by exfoliated MMT platelets.[21,22] In the UHMWPE/PP/PMM composites, the remarkable decrease of defects at boundaries between UHMWPE spherulites enhances the mechanical properties.

CONCLUSIONS

The WAXD analysis and TEM observation clearly indicate the formation of exfoliated and better intercalated structure for the UHMWPE/PP/PMM composites. The structure of PMM in the matrix is probably attributed to the synergistic effects of the complex intercalator (PEG/MDAB) on the intercalation and exfoliation for MMT.

The addition of a small amount of PM or PMM has been found able to reduce the melt viscosity of UHMWPE/PP (90/10) blend significantly, and PM shows better effect when compared with PMM. With 1 phr PM contents in the UHMWPE/PP (90/10) blend, the apparent melt viscosity is much lower than that of pure UHMWPE, and no pressure vibration occurs throughout the whole range of shear rate. With more addition of OMMT, more viscosity reduction of UHMWPE/PP (90/10) occurs.

The UHMWPE nanocomposites exhibit remarkable improvement of mechanical properties such as tensile strengths, elongation at break, and yield strength when compared with the matrix without clay. With higher clay loading, however, the impact strength drops for PM and MM based composites.

References

1. Prever, E. B.; Crova, M.; Costa, L.; Dallera, A.; Camino, G.; Gallinaro, P. Biomaterials 1996, 17, 873.
2. Engh, C. A.; Massin, P. Clin Orthop Relat Res 1989, 24, 141.
3. Kumar, P.; Oka, M.; Ikeuchu, K.; Shimizu, K.; Yamamuro, T.; Okumura, H.; Kotoura, Y. J Biomed Mater Res 1991, 25, 813.
4. Smith, P.; Lemstra, P. J. J Mater Sci 1980, 15, 505.
5. Smith, P.; Lemstra, P. J. Polymer 1980, 21, 1341.
6. Smith, P.; Lemstra, P. J. Makromol Chem 1979, 180, 2983.
7. Mackley, M. R.; Solbai, S. Polymer 1987, 28, 1115.
8. Mackley, M. R.; Solbai, S. Polymer 1987, 28, 1111.
9. Dumoulin, M. M.; Utracki, L. A.; Lara, J. Polym Eng Sci 1984, 24, 117.
10. Kyu, T.; Vadhar, P. J Appl Polym Sci 1986, 32, 5575.

11. Xie, M. J.; Liu, X. L.; Li, H. L. J Appl Polym Sci 2006, 100, 1282.
12. Alexandre, M.; Dubois, P. Mater Sci Eng 2000, 28, 1.
13. Ray, S. S.; Okamoto, M. Prog Polym Sci 2003, 28, 1539.
14. Wu, Q. Y.; Gao, W. P.; Hu, Y. L. J Appl Polym Sci 2001, 80, 2154.
15. Cullity, B. D. Element of X-ray Diffraction; Addison-Wesley: London, 1978.
16. Nam, P. H.; Kaneko, M.; Ninomiya, N.; Fujimori, A.; Masuko, T. Polymer 2005, 46, 7403.
17. Suprakas, S. R.; Kazunobu, Y.; Masami, O.; Kazue, U. Polymer 2003, 44, 857.
18. Ray, S. S.; Maiti, P.; Okamoto, M.; Yamada, K.; Ueda, K. Macromolecules 2002, 35, 3104.
19. Sinha, R. S.; Okamoto, K.; Okamoto, M. Macromolecules 2003, 36, 2355.
20. Wooster, T. J.; Abrol, S.; MacFarlane, D. R. Polymer 2005, 46, 8011.
21. Ma, J.; Zhang, S.; Qi, Z.; Li, G.; Hu, Y. J Appl Polym Sci 2002, 83, 1978.
22. Hambir, S.; Bulakh, N.; Jog, J. P. Polym Eng Sci 2002, 42, 1800.